Energy Fuels **2011,** *25,* 684–693 · DOI:10.1021/ef101307a
Published on Web 01/10/2011

energy&fuels
article

Investigation of the Diffuse Interfacial Layer of Superfine Pulverized Coal and Char Particles

Jiaxun Liu,[†,‡] Xiumin Jiang,[†] Xiangyong Huang,[†] Jun Shen,[†] and Shaohua Wu*[,‡]

[†]*School of Mechanical Engineering, Shanghai Jiao Tong University, Minhang District, Shanghai 200240, China, and* [‡]*School of Energy Science and Engineering, Harbin Institute of Technology, West Straight Street, Harbin 150001, China*

Received May 11, 2010. Revised Manuscript Received December 14, 2010

Superfine pulverized coal combustion is a new pulverized coal combustion technology that has better combustion stability, higher combustion efficiency, and lower NO_x and SO_2 emissions. In this paper, small-angle X-ray scattering (SAXS) measurements were utilized to calculate the diffuse interfacial thickness of superfine pulverized coal and char particles. Porod's law was applied to quantitatively analyze the SAXS curves with gray relational analysis (GRA) used for further investigation of the influencing factors on the thickness of the diffuse interfacial layer. Negative deviations from Porod's law of SAXS curves were found for all the coal samples, indicating the existence of diffuse interfacial layers in the grains. When considered in conjunction with coal pyrolysis experiments and Fourier transform infrared spectroscopy investigations, it is proposed that the interfacial layer is caused by the organic groups linked to the matrix of the coals. As the variation of interfacial thickness is so small, analysis of variance and multiple comparisons were applied to confirm the statistical significance. The effect of inorganic elements on the diffuse interfacial layer of coal particles was also studied using the demineralized samples. Final results indicate that the interfacial thickness of the superfine pulverized coal particles ranges from 0.23 to 0.66 nm and decreases with increasing coal quality and particle size. For the char particles, the interfacial thickness decreases with increasing pyrolysis temperature. Demineralized coal particles in the similar experiments show the same trends as the raw coals; however, the acid washing process increases the diffuse interfacial thickness. The findings from this work will help form the basis of, and provide guidance for, further studies on the chemical and combustion characteristics of superfine pulverized coal particles.

1. Introduction

Coal is the major energy resource in China.[1] Utility boilers consume about 27% of the total coal production, generate about 70% of the country's electricity, and emit the majority of pollutants into the atmosphere.[2] To meet the demand of combusting with high combustion efficiency and low pollutant emissions and to solve the problems of flame stability, slagging and char burnout, the use of superfine pulverized coal particle combustion has been proposed.[3,4] Previous research found that the combustion of superfine pulverized coal particles (particle diameter below 20 μm on average) has many advantages, such as better stability, higher combustion efficiency, and lower NO_x and SO_2 emissions, than combusiton using conventional techniques.[5−8] The structure of coal has long been the subject of intense interest and investigation.[9] This is in large part due to the importance of the pore structure to the passages of fluids in and out of coal, which naturally occur when coal is processed or burnt. The porosity and nature of coal surfaces may play a key role in many types of chemical reactions and in solvent transport during fluid extraction processes.[10] Hence, further study on the physical structure of superfine pulverized coal particles will enhance the understanding of the mechanisms involved in superfine pulverized coal particle combustion.

Small-angle X-ray scattering (SAXS) is a well-established method for the characterization of porous media with pore sizes in the range from 1 to 100 nm.[11] This technique, well adapted to study the spatial fluctuations of the electronic density inhomogeneities within a substance, was extensively applied to investigate the porous materials.[12] The application of SAXS to complex systems may overcome some limitations of other experimental techniques. For example, SAXS can detect both closed and open pores in porous materials, whereas adsorption techniques can only evaluate the open pores.[13]

*To whom correspondence should be addressed. Telephone: +86 451 8641 2628. E-mail: wush@hit.edu.cn.

(1) Li, Y. W.; Zhao, C. S.; Wu, X.; Lu, D. F.; Han, S. *Korean J. Chem. Eng*. **2007**, *24*, 319–327.
(2) Li, Z. Q.; Yang, L. B.; Qiu, P. H.; Sun, R.; Chen, L. Z.; Sun, S. Z. *Int. J. Energy Res*. **2004**, *28*, 511–520.
(3) Nakamura, M.; Takashi, K.; Kuwahara, M.; Watanabe, H.; Kitamura, R.; Tanaka, T. *International Conference on Power Engineering-97*, ICOPE-97: Tokyo; 1997; Vol. *2*, pp 453−458.
(4) Jiang, X. M.; Li, J. B.; Qiu, J. R. *Proceedings of the CSEE* **2000**, *20*, (in Chinese).
(5) Jiang, X. M.; Zheng, C. G.; Yan, C.; Liu, D. C.; Qiu, J. R.; Li, J. B. *Fuel* **2002**, *81*, 793–797.
(6) Jiang, X. M.; Zheng, C. G.; Qiu, J. R.; Li, J. B.; Liu, D. C. *Energy Fuels* **2001**, *15*, 1100–1102.
(7) Zhang, C. Q.; Jiang, X. M.; Wei, L. H.; Wang, H. *Energy Convers. Manage*. **2007**, *48*, 797–802.
(8) Fan, J. J.; Jin, J.; Zhang, J. M.; Zhang, Z. X. *J. Eng. Thermophys*. **2006**, *27*, 231–233 (in Chinese).
(9) Cooper, B. R.; Gruner., W. R.; Anderson, L. *Rev. Mod. Phys*. **1981**, *53*, 51–168.
(10) Nemmers, S.; Horne, D. K.; Bale, H. D. *J. Appl. Phys*. **1990**, *68*, 3178–3186.
(11) Rouquerol, J.; Avnir, D.; Fairbridge, C. W.; Everett, D. H.; Haynes, J. H.; Pernicone, N.; Ramsay, J. D. F.; Sing, K. S. W.; Unger, K. K. *Pure Appl. Chem*. **1994**, *66*, 1739–1758.
(12) Imelik, B.; Vedrine, J. C. *Catalyst Characterization Physical Techniques for Solid Materials*; Plenum Press: New York, 1994.

1.1. Application of SAXS Techniques to Coals and Chars. Since Bale and Schmidt[14] demonstrated theoretically that the surface fractal dimension (D_s) can be obtained using small-angle X-ray scattering (SAXS) measurements, there have been many studies on the D_s and the pore structure of coal. Bale et al.[14] developed a method for analyzing the high-Q region of a SAXS curve for porous scatterers in which the pore boundaries can be described by fractals and the fractal dimension of the lignite in the experiments was found to be about 2.56. Bodoev et al.[15] attempted to prepare active carbons starting from sapropelitic coals combining low-temperature modification and chemical activation. Surface areas were determined by BET (Brunauer−Emmett−Teller) and SAXS methods. It was shown that the results obtained with BET area determination can be confirmed by SAXS analysis. In this paper, FTIR spectroscopy was also applied to analyze new functional group formation and organic framework reorganization. Radlinski et al.[16] discussed the applicability of small-angle X-ray scattering and small-angle neutron scattering (SANS) techniques for determining the porosity, pore size distribution, and internal specific surface area in coals. This method can be used for any type of coal sample, from a thin slice to a representative sample of a thick seam. Mitropoulos et al.[17] characterized two highly volatile bituminous coal samples by adsorption and SAXS. Final results suggested that adsorption in conjunction with SAXS can provide information on the pore structure, the adsorption mechanism, and any swelling of the solid matrix upon adsorption. Snook et al.[18] utilized SAXS to study the fractal pore surfaces in Brown coal and found that the scattering pattern caused by the pore surfaces of dried coal may often be interpreted as arising from fractally rough surfaces. Larsen et al.[19] measured the fractal dimensionality of the pores in five Argonne Premium Coals using SAXS and found they varied between 2.35 and 2.87. They proposed that pores in coals were isolated and could be reached only by diffusion through the solid. Mitropoulos et al.[20] examined the effect of thermal treatment at a relatively high temperature on two bituminous coals by water adsorption and SAXS. The results suggested that the mesopore structure in both samples underwent a partial collapse. Nakagawa et al.[21,22] investigated the change in the surface fractal dimension of Witbank coal with heat treatment using SAXS. It was found that the D_s changes systematically depending on the temperature and the heating rate.

1.2. Application of SAXS To Study the Interfacial Layer. Ruland et al.[23] has shown that Porod's law may be modified to include the effect of negative deviations and had proposed methods to determine the density fluctuations and width of the diffuse interface used for pinhole collimation. Hashimoto et al.[24] estimated thickness of the domain-boundary interphase which was quantitatively calculated by analyzing a systematic deviation of the scattering curves at large angle tail from the Porod's law. They also found that the interfacial thickness was almost independent of the molecular weight covered in their latter studies.[25,26] Bjorkqvist et al.[27] determined the thickness of an oxide layer at the p+-type porous silicon interface by using SAXS and found that the thickness was a function of oxidation time. Koberstein et al.[28] determined the diffuse boundary thickness of polymers by SAXS and proposed a simple method from direct graphical analysis of slit-smeared intensity data, which was modeled by a sigmoidal-gradient model. Myers et al.[29] investigated the morphology of amorphous/semicrystalline nylon blends using SAXS, and their measurements of the diffuse boundary thickness showed a dependence on blend composition.

The present work elaborates the surface geometry of superfine coal particles using SAXS and the characteristics of the surface layer on the particles. Through the quantitative analysis of SAXS curves using Porod's law, it is proposed that the interfacial layer is caused by the organic groups linked to the matrix of the coals. Fourier transform infrared (FTIR) spectroscopy investigations of the organic groups of coal particles are used to test this proposition. Furthermore, SAXS studies of demineralized coals and chars from coal pyrolysis experiments in a fixed-bed reactor were also applied to validate this conclusion.

2. Experimental Section

2.1. Properties of Superfine Pulverized Coals. Shenhua (SH) and Neimenggu (NMG) coals of China were chosen for the experiments. The coal samples were pulverized into eight different mean particle sizes using a jet mill. The particle size distributions of the coals were analyzed by a Malvern MAM5004 Laser Mastersizer made in the U.K. The equivalent mean particle sizes of SH samples were 14.705, 17.439, 21.3, and 44.264 μm, whereas those of NMG samples were 12.561, 14.999, 25.862, and 52.778 μm. The properties of the coals are presented in Table 1. The ultimate analysis data were obtained on a LECO CHN 600 (U.S.) and a sulfur analyzer, and then the oxygen content was obtained by difference. The proximate analysis was done on a LECO MAC 500 (U.S.).

2.2. SAXS Analysis at the Shanghai Synchrotron Radiation Facility. The SAXS experiment was performed using synchrotron radiation as the X-ray source with a long-slit collimation system at the Shanghai Synchrotron Radiation Facility (SSRF). X-rays of 1.24 Å in wavelength were selected and focused to 1.2 (vertical) × 1.5 (horizontal) mm^2 at the detector with a camera length of 5417 mm. The energy range we applied is stable around 10 keV, and the energy resolution $\Delta E/E$ is 6.0×10^{-4} at 10 keV. The

(13) Li, Z. H.; Gong, Y. J.; Wu, D.; Sun, Y. H.; Wang, J.; Liu, Y.; Dong, B. Z. *Microporous Mesoporous Mater*. **2001**, *46*, 75–80.
(14) Bale, H. D.; Schmidt, P. W. *Phys. Rev. Lett*. **1984**, *53*, 596–599.
(15) Bodoev, N. V.; Gruber, R.; Kucherenko, V. A.; Guet, J. M.; Khabarova, T.; Cohaut, N.; Heintz, O.; Rokosova, N. N. *Fuel* **1998**, *17*, 413–418.
(16) Radlinski, A. P.; Mastalerz, M.; Hinde, A. L.; Hainbuchner, M.; Rauch, H.; Baron, M.; Lin, J. S.; Fan, L.; Thiyagarajan., P. *Int. J. Coal Geol*. **2004**, *59*, 245–271.
(17) Mitropoulos, A. C.; Stefanopoulos, K. L.; Kanellopoulos, N. K. *Microporous Mesoporous Mater*. **1998**, *24*, 29–39.
(18) Snook, I.; McMahon, P. *Langmuir* **1993**, *9*, 2726–223.
(19) Larsen, J. W.; Hall, P.; Wernett, P. C. *Energy Fuels* **1995**, *9*, 324–330.
(20) Mitropoulos, A. C.; Haynes, J. M.; Richardson, R. M.; Steriostis, T. A.; Stubos, A. K.; Kanellopoulos, N. K. *Carbon* **1996**, *34*, 775–781.
(21) Nakagawa, T.; Komaki, I.; Sakawa, M.; Nishikawa, K. *Fuel* **2000**, *79*, 1341–1346.
(22) Nakagawa, T.; Nishikawa, K.; Komaki, I. *Carbon* **1999**, *37*, 520–522.
(23) Ruland, W. *J. Appl. Crystallogr*. **1971**, *4*, 70–73.
(24) Hashimoto, T.; Todo, A.; Itoi, H.; Kawai, H. *Macromolecules* **1977**, *10*, 377–384.
(25) Hashimoto, T.; Fujimura, M.; Kawai, H. *Macromolecules* **1980**, *13*, 1237–1247.
(26) Hashimoto, T.; Fujimura, M.; Kawai, H. *Macromolecules* **1980**, *13*, 1660–1669.
(27) Bjorkqvist, M.; Salonen, J.; Laine, E. *J. Appl. Crystallogr*. **2003**, *36*, 740–743.
(28) Koberstein, J. T.; Morra, B.; Stein, R. S. *J. Appl. Crystallogr*. **1980**, *13*, 34–45.
(29) Myers, M. E.; Wims, A. M.; Ellis, T. S.; Barnes, J. *Macromolecules* **1990**, *23*, 2807–2814.

photon flux is 10^{12} photons/s at 10 keV, and the measurement of the smallest angle is 0.4 mrad. The scattered X-ray intensities were recorded using the imagery plate technology. The absorption of the sample and the background scattering were corrected. All the intensities of the samples are normalized by the data recorded from ionization chambers. All the SAXS data are converted in arbitrary scale.

2.3. Preparation of Demineralized Coal Samples. It is known that the present of mineral matter within the samples may have an influence on the determination of the pore size distribution from the SAXS technique.[16] To study the effect of inorganic matter on the diffuse interfacial layer of coal particles, acid washed coals were prepared from the raw coals in accordance with the Chinese Standard (GB/T 7560-2001). Approximately 6 g of coal was weighed into a glass beaker. Approximately 40 mL of 5 mol/L aqueous HCl solution was added to the coal, and the mixture was stirred and heated to 60 °C for approximately 50 min. The solution was filtered through a medium porosity sintered glass funnel. The coal was transferred to a Teflon beaker, and 40 mL of 49% HF was added. The solution was stirred and heated to 60 °C for approximately 50 min. The coal/HF solution was filtered and transferred to a glass beaker, and 2 mol/L HNO_3 was added. The mixture was stirred and heated to 70 °C for approximately 30 min. The coal/HNO_3 solution was diluted to 500 mL, filtered, and washed with of warm distilled water. The coal was transferred to a tared bottle and dried to a constant weight at 105 °C and used for pyrolysis studies.

2.4. Preparation of Chars. The investigations of coal pyrolysis were carried out in a fixed-bed reactor. In the experiments, the coal samples were heated in the pipe furnace by a programmed temperature controller under N_2 and CO_2 atmospheres. Gas release characteristics were analyzed by applying a Gasmet DX-4000 FTIR gas analyzer (Finland) to realize online measurement. The sketch of the experiment system is shown in Figure 1.

2.5. FTIR Analysis of Coal Particles. The Fourier transform infrared spectroscopy (FTIR) analyses were performed on an EQUNXO 55 FTIR spectrometer (Germany) using the potassium bromide (KBr) technique. A 2 mg portion of crushed coal was blended with 80 mg of KBr and crushed in an agate mortar. Each sample was analyzed in duplicate, and the spectrum from each analysis was derived by averaging 64 scans of the region of 4000−400 cm^{-1}.

2.6. ANOVA and GRA Methods Introdution. Because the variation of interfacial thickness is so small, we applied the analysis of variance (ANOVA) and multiple comparisons to confirm the statistical significance. This method has been widely used in biological fields, which is very useful for error analysis and statistical significance confirmation. Gray system theory describes the course of looking for the regularity of a variable by dealing with raw data. Gray relational analysis (GRA) is part of the gray system theory, which is useful for dealing with poor, incomplete, and uncertain information and complicated interrelationships between multiple factors and variables. We think it is suitable to apply gray system theory to identify the influencing factors of interfacial thickness.

Table 1. Ultimate and Proximate Analyses of the SH and NMG Coals

	proximate analysis (wt %) (ad)		ultimate analysis (wt %) (ad)	
SH	moisture	11.5	C	63.13
	volatile	24.22	H	3.62
	ash	10.7	O	9.94
	fixed carbon	53.58	N	0.70
			S	0.41
NMG	moisture	14.72	C	54.82
	volatile	35.69	H	4.39
	ash	10.64	O	14.58
	fixed carbon	38.95	N	0.63
			S	0.22

3. Results and Discussion

Through our previous studies, it is known that the surface morphology of coal particles includes external (particle shape,[30] surface roughness,[31] etc.) and internal morphology[32] (pore size distribution, pore surfaces, tortuosity, etc.). Superfine pulverized coal has a complex surface structure that is generally considered as being distributed in two components, suggesting that there is a diffuse interfacial layer located between the pores and the matrix. A schematic illustration of coal surface morphology is shown in Figure 2. An accurate description of coal surfaces is crucial to the development of the superfine pulverized coal combustion technique. The SAXS technique has been used in this paper to calculate the interfacial thickness of superfine pulverized coals and chars.

3.1. Porod's Law Analysis of Superfine Pulverized Coal Particles. *3.1.1. A Negative Deviation from Porod's Law.* It is well known that only scattering by ideal two-phase systems with sharp boundaries obeys Porod's law.[33] It is known that Porod's law predicts a decrease in intensity proportional to the reciprocal fourth power of s

$$\lim_{s \to \infty} [I_p(s)] = \frac{K_p}{s^4} \quad (1)$$

where $s = 2 \sin(\theta) \lambda^{-1}$ and K_p is the so-called Porod law constant.[33]

The scattering intensity in the Porod region after removing contributions due to density fluctuations within the phases is given by

$$I_{obs}(s) = I_p(s) H^2(s) \quad (2)$$

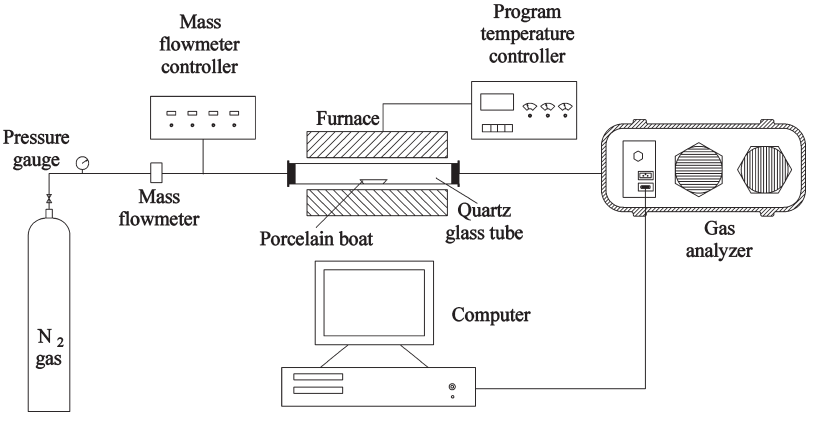

Figure 1. Sketch of the fixed-bed reactor experimental system.

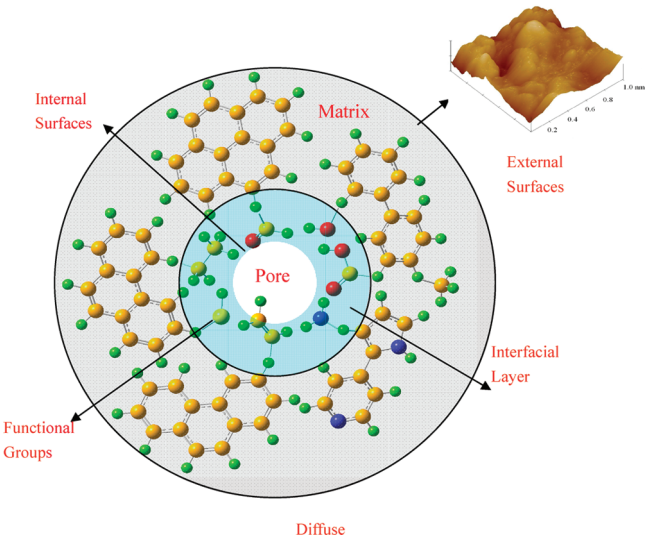

Figure 2. Schematic illustration of coal surface morphology.

where $I_p(s)$ is the Porod law intensity and $H^2(s)$ is the Fourier transform of the autocorrelation of the smoothing function. The smoothing function for the sigmoidal-gradient model is Gaussian, and thus, $H(s)$ is given by[28]

$$H(s) = \exp(-2\pi^2\sigma^2 s^2) \tag{3}$$

where σ is the standard deviation of the Gaussian smoothing function and is a measure of the transition layer width. The corresponding Porod law relation becomes[28]

$$I_{obs}(s) = (K_p/s^4)\exp(-4\pi^2\sigma^2 s^2) \tag{4}$$

It can then be used to determine diffuse boundary widths in the following form.

$$\ln(I_{obs}(s)s^4) = \ln K_p - 4\pi^2\sigma^2 s^2 \tag{5}$$

This is always used for the pinhole collimation system, and the diffuse boundary widths can be determined in plots ln $(I_{obs}(s)s^4)$ versus s^2.

The slit collimation has advantages over pinhole collimation, such as higher intensity, higher resolving power, and lower parasitic scattering. The inherent disadvantage of slit collimation is that the resultant scattering intensity is smeared. Numerous methods are available for desmearing the experimental scattering curves.[28]

An approximation for the slit-smeared intensity has been proposed by Bonart and Muller (1974).[34] From this approximation, the slit-smeared intensity is given by[34]

$$J(s) = 2\int_0^\infty W_l(u)I_{obs}(s^2+u^2)^{1/2}\,du \tag{6}$$

where $J(s)$ is the smeared intensity, $W_l(u)$ is the slit-length weighting function, and u is an arbitrary variable of integration.

Considering only negative deviations from Porod's law, it is found that

$$J(s) = 2\int_0^\infty W_l(u)I_p(s^2+u^2)^{1/2}H^2(s^2+u^2)^{1/2}\,du \tag{7}$$

For many experimental slit geometries, a Gaussian distribution function is applied to approximate the slit-length weighting function, which is shown as[28]

$$W_l(u) = W_l(0)\exp(-p^2u^2) \tag{8}$$

where p is related to the standard deviation of the Gaussian distribution and $W_l(0)$ is a normalization constant. Thus, the smeared intensity may be given as

$$J(s) = 2W_l(0)K_p\exp(p^2s^2)\int_0^\infty \frac{\exp[-(p^2+4\pi^2\sigma^2)(s^2+u^2)^2]}{(s^2+u^2)^2}\,du \tag{9}$$

One can obtain[23]

$$J(s) = (K'/s^3)\exp(p^2s^2)\times[(1-8\pi^2\alpha^2s^2)\mathrm{erfc}(2\pi\alpha s)+4\sqrt{\pi}\alpha s\exp(-4\pi^2\alpha^2s^2)] \tag{10}$$

where erfc is the complementary error function, $\alpha = [\sigma^2+(p/2\pi)^2]^{1/2}$, and $K' = W_l(0)K_p\pi/2$. If values of αs are very small, by expanding the exponential function, eq 10 may be approximated by

$$\begin{aligned} J(s) &\approx (K'/s^3)\exp(p^2s^2)\times[(1-8\pi^2\alpha^2s^2)] \\ &\approx (K'/s^3)\exp(p^2s^2)\exp(-8\pi^2\alpha^2s^2) \\ &= (K'/s^3)\exp(p^2s^2-8\pi^2\alpha^2s^2) \\ &= (K'/s^3)\exp(-4\pi^2\alpha^2s^2) \end{aligned} \tag{11}$$

Expressions of the form eq 11 will then be valid for finite slit-length values of p. It is known that q is the scattering vector, $4\pi\lambda^{-1}\sin(\theta)$, and α is a parameter related to the interface thickness. $s = q/2\pi$, and it can be described by[26]

$$\ln[q^3J(q)] = \ln K' - \alpha^2q^2 \tag{12}$$

where q is the scattering vector, $4\pi\lambda^{-1}\sin(\theta)$, $J(q)$ is the slit-smeared background-corrected scattering intensity, and K' is called the Porod constant.

Thus, for an ideal two phase-system, the slope of $\ln[q^3J(q)]$ plotted versus q^2 at high values of the scattering vector is expected to be zero. It has been pointed that the increase of thermal density will cause the electronic density fluctuations in the interior of the scattering particles, which can enhance the high-q scattering intensity. Therefore, the SAXS will show a positive deviation from Porod's law. On the other hand, for a nonideal two-phase system with a diffuse interfacial layer between the two phases, which causes a depletion of scattering,

(30) Liu, J. X.; Jiang, X. M.; Huang, X. Y.; Wu, S. H. *Energy Fuels* **2010**, *24*, 844–855.
(31) Liu, J. X.; Jiang, X. M.; Huang, X. Y.; Wu, S. H. *Fuel* **2010**, *89*, 3884–3891.
(32) Liu, J. X.; Jiang, X. M.; Huang, X. Y.; Wu, S. H. *Energy Fuels* **2010**, *24*, 3072–3085.
(33) Porod, G. *Kolloid-Z.* **1951**, *124*, 83–114 (in German).
(34) Bonart, R.; Muller, E. H. *J. Macromol. Sci., Part B: Phys.* **1974**, *B10*, 177–189.

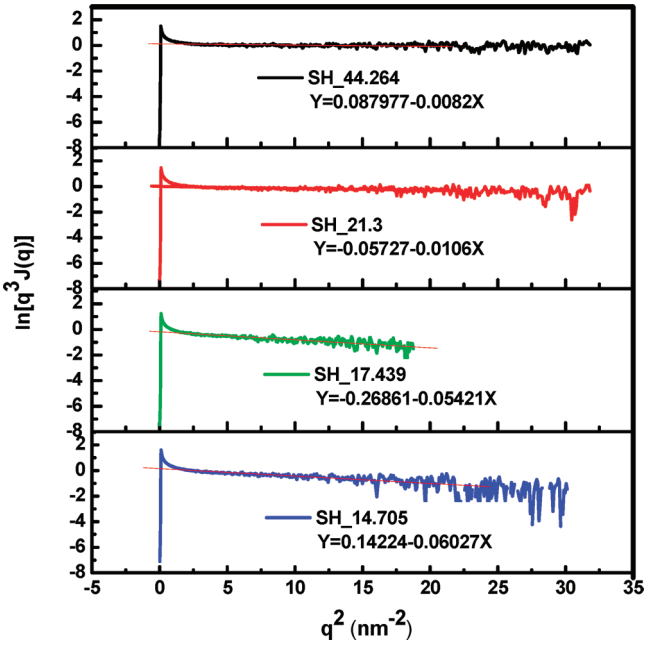

Figure 3. SAXS data plotted as $\ln[q^3J(q)]$ versus q^2 for SH coal specimens. X and Y in the figure represent the values of q^2 and $\ln[q^3J(q)]$, respectively.

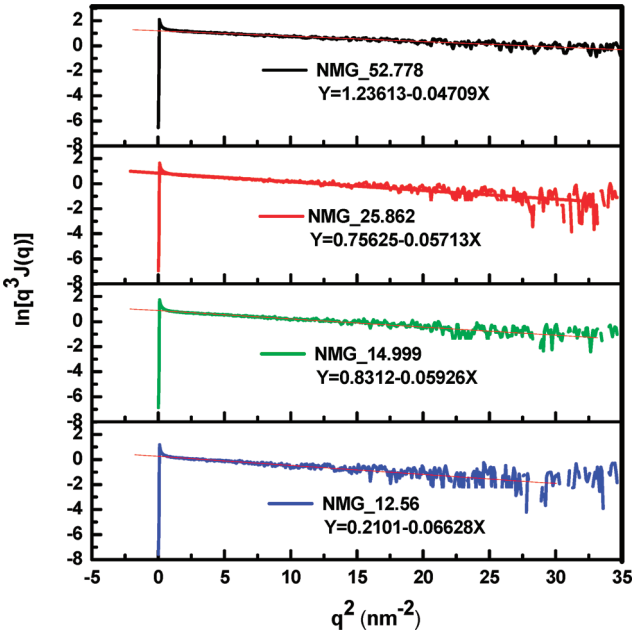

Figure 4. SAXS data plotted as $\ln[q^3J(q)]$ versus q^2 for NMG coal specimens. X and Y in the figure represent the values of q^2 and $\ln[q^3J(q)]$, respectively.

especially at a high scattering angle, it will lead to a negative deviation from Porod's law.[35]

In Figures 3 and 4, plots of $\ln[q^3J(q)]$ versus q^2 are displayed for NMG and SH coals. It is observed that Porod's law is not satisfied and the curve in the high-q region shows a negative slope, that is, a negative deviation from Porod's law for both NMG and SH coals. This suggests that the electron density does not change abruptly but varies gradually over a certain range of distances between the two phases in each sample. This range refers to a diffuse interfacial layer.

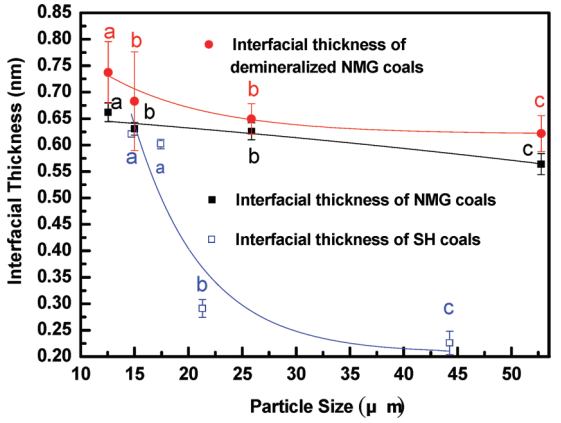

Figure 5. Influence of the coal particle size on the diffuse interfacial thickness of coals. The lower-case letters in the figure (a, b, c, etc.) represent the different significance levels ($P = 0.05$).

A linear relation with a negative slope of $\ln[q^3J(q)]$ versus q^2 at high values of the scattering vector can be fitted using formula 12, and the average thickness E of the interfacial layer can be calculated as[25]

$$E = (2\pi)^{0.5}\alpha \tag{13}$$

The σ for each coal sample was calculated by determining the slope of the best-fit line through the data points using linear regression, which is also shown in Figures 3 and 4. By applying the above formulas 12 and 13, E can be obtained and is summarized in Figure 5. The results indicate that, with the decrease of the particle size, the diffuse interfacial thickness of SH specimens increases from 0.23 to 0.62 nm, whereas that of NMG specimens increases from 0.56 to 0.66 nm. Furthermore, it can be observed that the thickness of the interfacial layer in NMG coal particles is larger than that of SH coal. From Table 1, it can be seen that the carbon content of SH specimens is higher than that of NMG coals; that is, the maturity of SH coals is higher. It is proposed that it is related to the organic groups linked to the matrix of the coals, as explained later in the organic group analysis section (section 3.2).

To confirm the statistical significance, we applied the analysis of variance (ANOVA) and multiple comparisons to the thickness in Figure 5 with error bars added. First, we carried out the one-factor analysis of variance and found that influences of particle sizes of SH and NMG specimens on the interfacial thickness are both significant (the test statistics of SH specimens is $F_{3,8,0.05} = 585.24$, whereas that of NMG is 16.40, which are all larger than the standard $F_{0.05}$ (3, 8) = 4.066). One-factor ANOVA suggests that the particle size has significant influences on the interfacial thickness. Therefore, to investigate the significance of differences between particle sizes, multiple comparisons were used. There are numerous methods of multiple comparisons, including the least significant difference (LSD), Tukey method, Newman method, and Duncan method.[36] In this paper, we adopted the Duncan multiple range test. The lower-case letters (a, b, c, etc.) show the different significance levels

(35) Chen, Z. J.; Wang, W.; Cai, Q.; Chen, X.; Wu, Z. H.; Li, R. P.; Che, C. Q.; Pan, W. *Chin. Phys. Soc.* **2008**, *57*, 5793–5799 (in Chinese).

(36) Du, R. S. *Biostatistics* (in Chinese); Higher Education Press: Beijing, 2004.

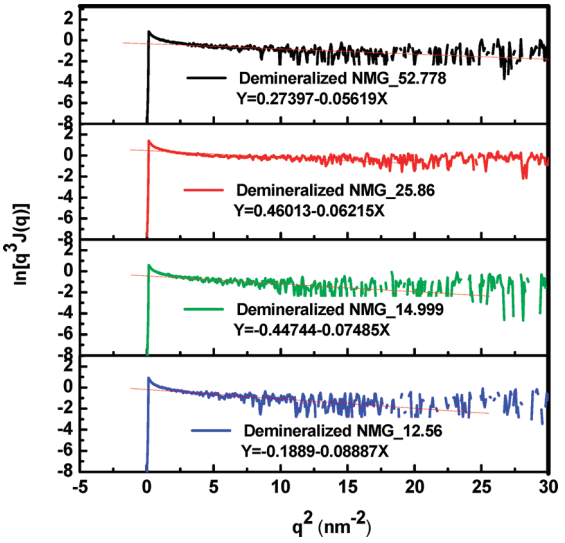

Figure 6. SAXS data plotted as $\ln[q^3J(q)]$ versus q^2 for demineralized NMG coal specimens. X and Y in the figure represent the values of q^2 and $\ln[q^3J(q)]$, respectively.

($P = 0.05$). Hence, from the multiple comparisons in Figure 5, it can be concluded that the differences between the diffuse interfacial thickness of both SH and NMG coals are notable.

3.1.2. Influence of Mineral Matter within the Samples on the Interfacial Layer Thickness from the SAXS Technique. It is known that the presence of mineral matter within the samples may have an influence on the determination of pore size distribution from the SAXS technique. To study the effect of inorganic elements on the diffuse interfacial layer of coal particles, acid washed coals were prepared from the raw coals. In Figure 6, plots of $\ln[q^3J(q)]$ versus q^2 are displayed for demineralized NMG coals. It can be seen that the curve in the high-q region also shows a negative slope, that is, a negative deviation from Porod's law for demineralized coals. By applying the above formulas 12 and 13, E could be obtained and is summarized in Figure 5. The results show that, with the increase of the particle size, the diffuse interfacial thickness of demineralized NMG specimens decreases from 0.74 to 0.62 nm. Furthermore, it can be observed that all the interfacial thicknesses of demineralized NMG specimens are larger than those of the raw NMG coals. There may be two reasons. First, Radlinski et al.[16] concluded that the scattering occurs predominantly between the polyaromatic sheets and intercalated inorganic matter based on SAXS and SANS contrast considerations. The micropores appear to be significantly clogged with nearly molecular-sized particles of inorganic matter, probably clays. It has been pointed that the increase of thermal density, such as the evolution of the inorganic matter in the matrix, will cause the electronic density fluctuations in the interior of the scattering particles, which can enhance the high-q scattering intensity. Therefore, it is concluded that the presence of inorganic matter within the particles will decrease the diffuse interfacial thickness. Second, demineralization and additional pyrite removal by diluted HNO_3 will cause some coal oxidation and some nitrate groups were intermingled to the samples during the HNO_3 acid washing process. Thus, the acid washing process will increase the thickness. Hence, in our opinion, the effects of the acid washing process on the characteristics of raw coals cannot be neglected here on studying the diffuse interfacial thickness. In general, the exclusion of inorganic matter and the addition of extra functional groups to the samples during the acid washing process will both increase the diffuse interfacial thickness of coal particles. The extent to which the interfacial thickness may be affected by these processes requires further study.

Table 2. Influencing Factors of Diffuse Interfacial Thickness

	carbon (%)	volatile (%)	mean diameter (μm)	interfacial thickness (nm)
SH	66.395	30.171	44.264	0.226 ± 0.022
	61.05	30.199	21.300	0.291 ± 0.017
	69.89	28.692	17.439	0.602 ± 0.009
	69.485	29.843	14.705	0.621 ± 0.006
NMG	55.21	35.895	52.778	0.564 ± 0.020
	52.265	36.062	25.862	0.626 ± 0.016
	55.06	35.062	14.999	0.631 ± 0.012
	57.63	35.274	12.561	0.662 ± 0.018

3.1.3. Gray Relational Analysis of Factors Influencing the Diffuse Interfacial Thickness. The gray system theory proposed by Deng[37] has been widely applied to various fields, such as multiple attribute decision-making problems[38] and laser cutting parameters.[39] It has been proven to be useful for dealing with poor, incomplete, and uncertain information. Gray relational analysis (GRA) is part of gray system theory, which is suitable for solving problems with complicated interrelationships between multiple factors and variables.[40] The gray theory makes use of relatively small data sets and does not demand strict compliance to certain statistical laws, simple or linear relationships among the observables. It is suitable to apply gray system theory to the identification of influencing factors of fractal dimensions.[32]

The GRA is a quantitative analysis to explore the similarity and dissimilarity among factors in developing a dynamic process. The theory proposes a dependence to measure the correlation degree of factors; the more similarities develop, the more factors correlate. It uses the gray relational grade to measure the relational degree of factors.[41] The analysis procedure was described in detail elsewhere.[42,43]

The influencing factors of the diffuse interfacial thickness were analyzed by the gray relational analysis method, as listed in Table 2. As fixed carbon is calculated by difference, it soaks up the errors for the other proximate analyses. We used the carbon analysis instead of fixed carbon in the paper. The parameters of carbon contents and volatile matter were chosen to represent the quality of coal samples. The diffuse interfacial thickness obtained by formula 13 in Figures 3 and 4 was used as a reference sequence. The carbon analysis, volatile matter, and mean diameter of the coal particles were affirmed as comparison sequences. An equalization approach was used in processing the data to obtain a dimensionless eigenvector matrix. The index for distinguishability was set to 0.5, and gray relational sequences considering the influence of carbon contents, volatile matter, and mean diameter of the coal particles on the diffuse interfacial thickness were obtained (see Table 3).

(37) Deng, J. *Syst. Control Lett.* **1982**, *1*, 288–294.
(38) Caydas, U.; Hascalik, A. *Opt. Laser Technol.* **2008**, *40*, 987–994.
(39) Chang, T. C.; Lin, S. J. *J. Environ. Manage.* **1999**, *56*, 247–257.
(40) Kuo, Y.; Yang, T.; Huang, G. W. *Comput. Ind. Eng.* **2008**, *55*, 80–93.
(41) Kung, C. Y.; Wen, K. L. *Decis. Support Syst.* **2007**, *43*, 842–852.
(42) Han, X. X.; Jiang, X. M.; Liu, J. G.; Wang, H. *Oil Shale* **2006**, *23*, 99–109.
(43) Wang, H.; Jiang, X. M.; Liu, J. G.; Lin, W. G. *Energy Fuels* **2007**, *21*, 1924–1930.

Table 3. Results of Gray Relational Analysis on Diffuse Interfacial Thickness

influencing factors	gray relational grade
carbon (X_1)	0.783
volatile (X_2)	0.812
mean diameter (X_3)	0.603
sequence	$X_2 > X_1 > X_3$

From the order, the degree of the effect of comparison sequences on the reference sequence can be worked out.

Generally, gray relational grade $X > 0.9$ indicates a marked influence, $X > 0.8$ a relatively marked influence, $X > 0.7$ a noticeable influence, and $X < 0.6$ a negligible influence.[44] On the basis of the above calculation results, volatile matter is the variable relatively markedly influencing the interfacial thickness, whereas carbon content is a noticeable influence. The influence of the coal particle size cannot be excluded and is worthy of further investigation. On the basis of this conclusion, further studies on the diffuse interfacial thickness of superfine pulverized coal particles were carried out.

3.2. Analysis of the Diffuse Interfacial Thickness of Superfine Pulverized Coal Particles. *3.2.1. Influencing Factors of the Coal Quality on the Diffuse Interfacial Thickness.* With the increase of the coal carbon content, the volatile matter decreases due to the decline of the amount of the organic groups, such as branched alkyl groups and functional groups. It is proposed that the interfacial layer is caused by the organic groups linked to the matrix of the coals. Thus, the thickness of the interfacial layer should decrease with the quality of the coals.

3.2.1.1. Pyrolysis of Original Coal Samples. To validate this assumption, investigations of coal pyrolysis in a fixed-bed reactor were carried out. In the experiments, the NMG coal samples with the particle sizes of 12.561 and 25.862 μm (the results of other particle sizes that have the similar trends are not shown here) were chosen to be heated in the pipe furnace by a programmed temperature controller under nitrogen and CO_2 atmospheres. Demineralized NMG_12.561 coals were also utilized in the pyrolysis experiments. Gas release characteristics were analyzed by applying a Gasmet DX-4000 FTIR gas analyzer (Finland) to realize online measurement. In the experiments, 0.4 g samples were loaded in the porcelain boat, and the temperatures were heated to 400, 600, and 800 °C with the same heating rate (20 °C/min). The rate of the nitrogen stream was kept stable at 3 L/min. The main products during pyrolysis of the NMG_12.561 coals in a N_2 atmosphere are shown in Figure 7. It is known that the organic sulfur-containing species in coal are presented as both aliphatic sulfur-containing side chains (thioethers) and heteroatoms in single-ring or multiring aromatic clusters.[45] From Figure 7, it can be seen that the release of SO_2 presents peaks around 450 °C, which is formed in the pyrolysis of organic sulfur and partial pyrite pyrolysis. Hence, there is still some organic sulfur left in the chars formed at 400 °C. The largest release of CH_4 appears at about 500 °C. In general, the formation of CH_4 at low temperature is caused by the cleavage of side chains of aliphatic hydrocarbons and alkyl groups.[46] Therefore, there is still some side chains of aliphatic hydrocarbons and alkyl groups left in the chars formed at 400 °C. Furthermore, from about 200 °C,

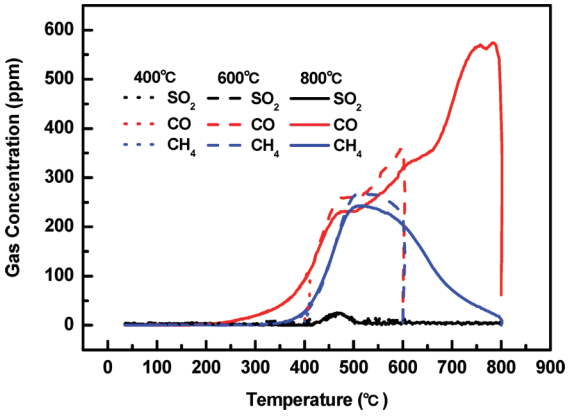

Figure 7. Yield of main gaseous products during the pyrolysis of coals.

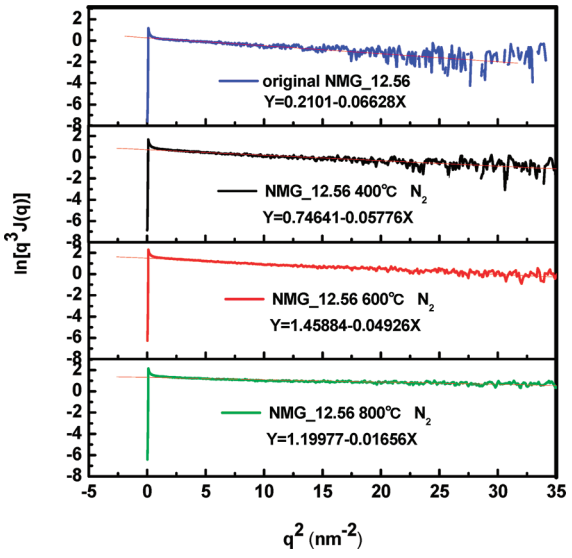

Figure 8. SAXS data plotted as $\ln[q^3J(q)]$ versus q^2 for NMG_12.561 coal chars in a N_2 atmosphere. X and Y in the figure represent the values of q^2 and $\ln[q^3J(q)]$, respectively.

CO begins to release, and with increasing temperature, the yield of CO also increases. During the pyrolysis of coals, CO originates mainly from the cleavage of hydroxyl groups, ether links, and oxygen heterocyclic rings.[47] As a result, it suggests that there are still hydroxyl groups left in the chars formed at 400 and 600 °C and there may be only a small quantity of organic groups left in the chars formed at 900 °C.

Plots of $\ln[q^3J(q)]$ versus q^2 are displayed for NMG_12.561 and NMG_25.862 coal and chars in Figures 8−11. The σ for each char sample was calculated by determining the slope of the best-fit line through the data points using linear regression, which is also shown in Figures 8−11. By applying the above formula 13, the interfacial thickness (E) could be obtained and is summarized in Figure 12. Analysis of variance (ANOVA) and the Duncan multiple range test were used to confirm the statistical significance. The test statistics of NMG_12.561 chars in a N_2 atmosphere is $F_{3,8,0.05} = 18.92$, whereas that in a CO_2 atmosphere is 62.29, which are all larger than the standard $F_{0.05}(3, 8) = 4.066$. This indicates that the influence of temperatures on the interfacial thickness is significant. It can

(44) Fu, C. Y.; Zheng, J. S.; Zhao, J. M.; Xu, W. D. *Corros. Sci.* **2001**, *43*, 881–889.
(45) Calkins, W. H. *Energy Fuels* **1987**, *1*, 59–64.
(46) Cui, Y. P.; Qin, L. L.; Du, J.; Chang, L. P. *Coal Chem. Ind.* **2007**, *2*, 10–15 (in Chinese).
(47) Zhao, L. H.; Guo, H. Q.; Ma, Q. L. *Coal Convers.* **2007**, *30*, 5–9 (in Chinese).

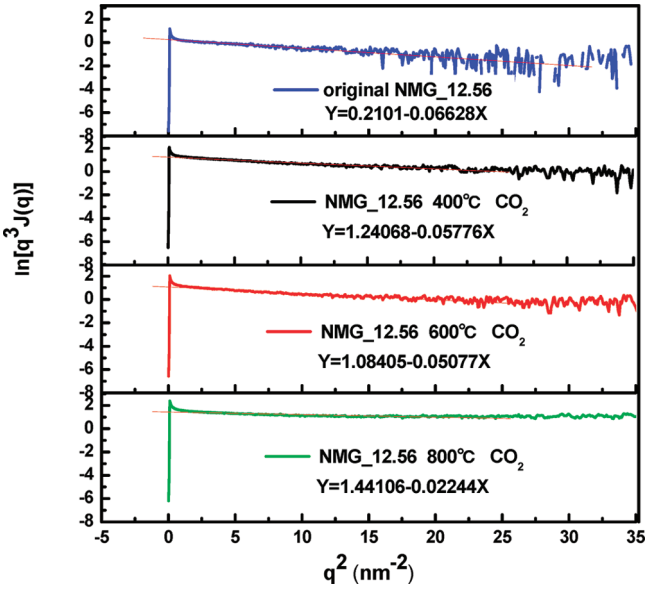

Figure 9. SAXS data plotted as $\ln[q^3J(q)]$ versus q^2 for NMG_12.561 coal chars in a CO_2 atmosphere. X and Y in the figure represent the values of q^2 and $\ln[q^3J(q)]$, respectively.

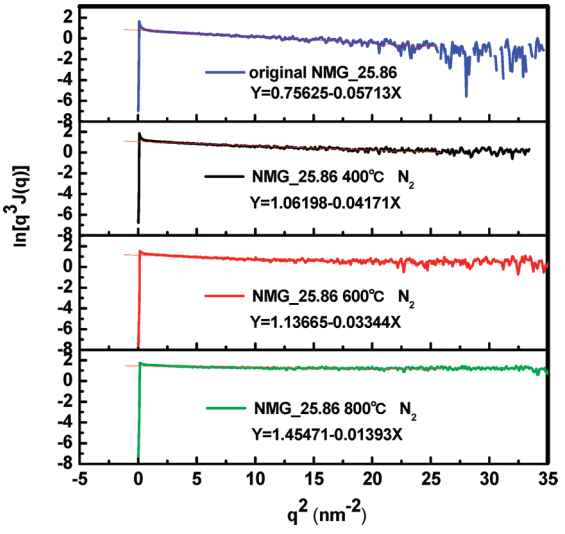

Figure 10. SAXS data plotted as $\ln[q^3J(q)]$ versus q^2 for NMG_25.862 coal chars in a N_2 atmosphere. X and Y in the figure represent the values of q^2 and $\ln[q^3J(q)]$, respectively.

be observed that the differences between the extrema are quite significant. It can also be seen that, for both chars formed in N_2 and CO_2 atmospheres, the interfacial thickness decreases with the increase of the temperature. Furthermore, all the interfacial thicknesses of NMG chars formed in a CO_2 atmosphere are thinner than the chars formed in a N_2 atmosphere. It is known[48] that replacing N_2 with CO_2 can enhance the volatile matter releasing rate greatly, even at 480 °C, and the volatile matter yield in a CO_2 atmosphere is greater than those in a N_2 atmosphere due to the gasification effect of CO_2. Thus, the functional groups left in the chars formed in a CO_2 atmosphere are less than those of the N_2 atmosphere chars. Hence, the interfacial thickness of NMG CO_2 atmosphere chars is thinner. It is thought that this is further evidence that the interfacial

(48) Duan, L. B.; Zhao, C. S.; Zhou, W.; Qu, C. R.; Chen, X. P. *Energy Fuels* **2009**, *23*, 3826–3830.

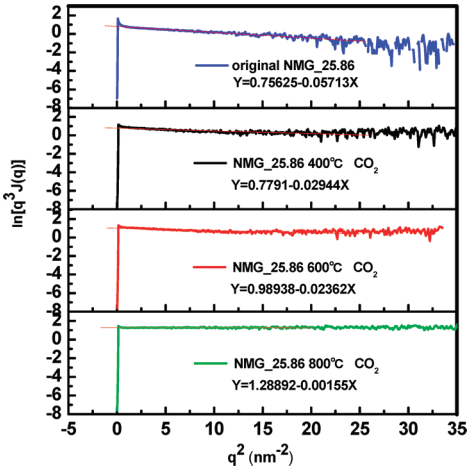

Figure 11. SAXS data plotted as $\ln[q^3J(q)]$ versus q^2 for NMG_25.862 coal chars in a CO_2 atmosphere. X and Y in the figure represent the values of q^2 and $\ln[q^3J(q)]$, respectively.

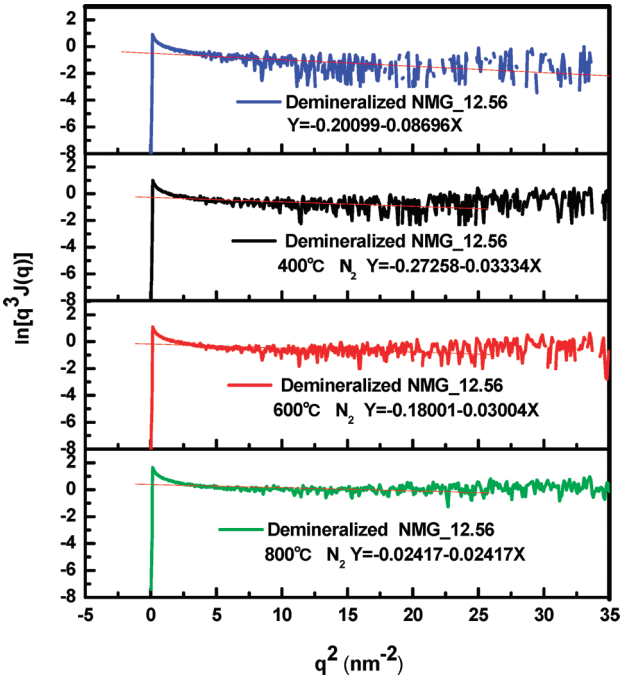

Figure 12. SAXS data plotted as $\ln[q^3J(q)]$ versus q^2 for demineralized NMG_12.561 coal chars in a N_2 atmosphere. X and Y in the figure represent the values of q^2 and $\ln[q^3J(q)]$, respectively.

layer of the coal particles is caused by the organic groups linked to the matrix. The conclusion drawn is that, with increasing pyrolysis temperature, there will be fewer organic groups left within the samples, which may result in the decrease of the interfacial thickness. With increasing rank, the volatile matter decreases (fewer organic groups), causing the decrease of the interfacial thickness.

3.2.1.2. Pyrolysis of Demineralized Coal Samples. To study the effect of inorganic elements on the diffuse interfacial layer of coal chars, demineralized NMG_12.561 coal particles were prepared for pyrolysis experiments. In Figures 13 and 14, plots of $\ln[q^3J(q)]$ versus q^2 are displayed for demineralized NMG coal chars. It is known that the curve in the high-q region also shows a negative slope, that is, a negative deviation from Porod's law for demineralized coal chars. By applying the above formulas 12 and 13, E could be obtained and

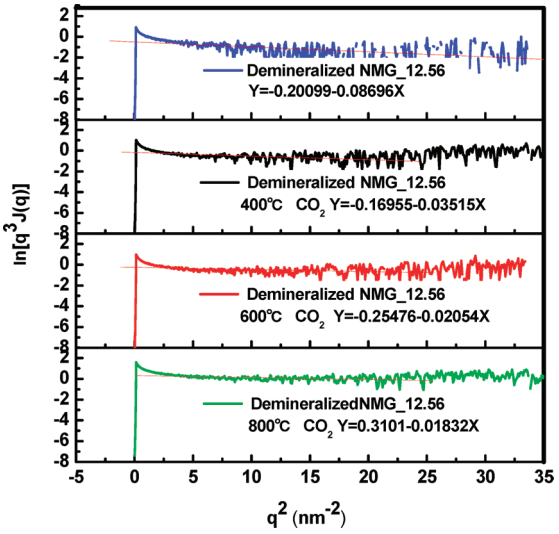

Figure 13. SAXS data plotted as $\ln[q^3J(q)]$ versus q^2 for demineralized NMG_12.561 coal chars in a CO_2 atmosphere. *X* and *Y* in the figure represent the values of q^2 and $\ln[q^3J(q)]$, respectively.

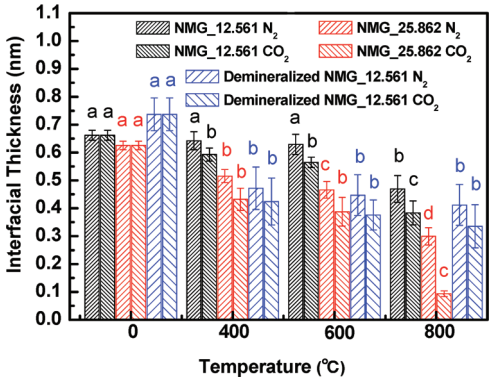

Figure 14. Influence of the temperature on the diffuse interfacial thickness of coal chars. The lower-case letters in the figure (a, b, c, etc.) represent the different significance levels ($P = 0.05$).

is summarized in Figure 12. The results show the same trend as that with the increase of the temperature; the diffuse interfacial thickness of demineralized NMG specimens decreases from 0.74 to 0.41 nm for N_2 atmosphere chars and from 0.74 to 0.34 nm for CO_2 atmosphere chars. It is also observed that all the interfacial thicknesses of demineralized NMG chars formed in a CO_2 atmosphere are thinner than the chars formed in a N_2 atmosphere. Furthermore, all the interfacial thicknesses of demineralized NMG_12.561 coal chars are thinner than those of the corresponding NMG_12.561 coal chars formed in the same temperature. The presence of inorganic elements may alter some of the coal properties, such as its swelling behavior.[49] Moreover, the removal of nonporous inclusions may affect the porosity, which can decrease the diffusion limitations for the expulsion of gaseous products.[50] These reasons lead to the increase of the yield of gaseous products for demineralized samples. Thus, the amounts of functional groups left in the coal chars become less, causing the decrease of the interfacial thickness. This phenomenon provides further evidence to support our assumption that the

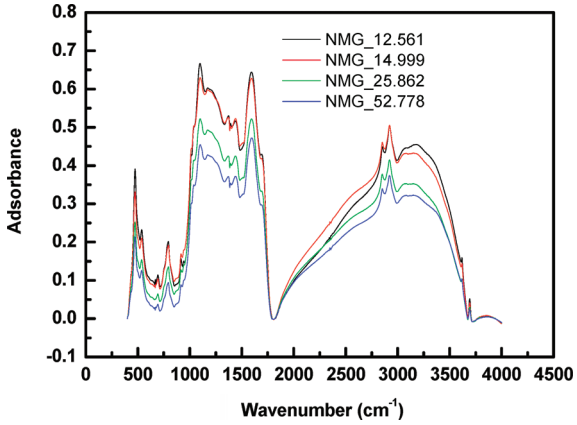

Figure 15. FTIR spectra of NMG coal specimens.

interfacial layer of the coal particles is caused by the organic groups linked to the matrix.

3.2.2. Influencing Factors of Coal Particle Size on the Diffuse Interfacial Thickness. Coal is a cross-linked molecule with high molecular weight.[51] The kernel of the coal structure is the aromatic ring. The whole coal macromolecule includes the skeleton, which is constituted by several similar basic structural units connected through bridging bonds. This skeleton is the matrix. Therefore, the mean diameter of coal particles increases with the increasing size of the skeleton molecule; that is, more basic structural units are connected in the coal macromolecule, the larger the mean coal diameter is. There are also some small molecular phases in macromolecules of coals.

Jestin et al.[52] performed a SANS study on emulsions made with dilute asphaltene solutions in xylene and at various pH conditions. In their work, three different asphaltene fractions, recovered from the same crude by precipitation with pentane, heptanes, or octane, were used to prepare the emulsions. With increasing precipitant carbon chain length, the authors observed an increase in emulsion film thickness, accompanied by a decrease in the calculated asphaltene composition within the films.[53] This is because the precipitant matters (pentane, heptanes, or octane) substitute some of the asphaltene and constitute the interfacial film. The longer the precipitant carbon chain length is, the larger the film thickness is. There is a similar situation in our study. It is proposed that the interfacial layer is caused by the organic groups linked to the matrix of coals, so with increasing the amounts and the chain length of organic groups, the interfacial layer thickness will increase.

The effect of particle size on the functional groups of the coal surfaces was studied using the diffuse reflection FTIR spectra. The FTIR spectra of NMG coals with different particle sizes are presented in Figure 10. The peak shapes of the coals are basically similar; however, the intensities, which represent the amounts of the functional groups, seem quite different. The hydroxyl group (−OH) stretching bands between 3000 and 3700 cm^{-1} are observed in Figure 15. It is known that the intensity of the OH stretching band decreases with increasing the particle size. Further investigation[54] indicated that the contents of hydroxyl groups,

(49) Bexley, K.; Green, P. D.; Thomas, M. K. *Fuel* **1986**, *65*, 47–53.
(50) Ahmad, T.; Awan, I. A.; Nisar, J.; Ahmad, I. *Energy Convers. Manage.* **2009**, *50*, 1163–1171.
(51) Hu, H. X.; Li, X. C.; Fang, Z. M.; Wei, N.; Li, Q. S. *Energy* **2010**, *35*, 2939–2944.
(52) Jestin, J.; Simon, S.; Zupancic, L.; Barre, L. *Langmuir* **2007**, *23*, 10471–10478.
(53) Verruto, V. J.; Kilpatrick, P. K. *Langmuir* **2008**, *24*, 12807–12822.

especially those of OH−π, OH−OH, and OH−ether, increase as the particle size decreases. The aliphatic C−H stretching vibration bands for coal samples are displayed in the range of 2800−3000 cm^{-1}. Further study also shows that the contents of C−H groups, such as $-CH_3$ and $-CH_2$, increase as the particle size decreases. The functional groups of the 1800−1000 cm^{-1} region for coal samples are complicated, including conjugated C=O, aromatic C=C, and C−O−R structures. The intensities of these stretches are also shown to decrease with increasing the particle size. This trend is a reflection of the effect of mechanical chemistry. It is known that there are mechanochemical effects and mechanical activations of substances in comminuting devices. The processes of melting and subsequent inevitable solidification (crystallization or amorphization) of the particles are important for mechanochemistry in a general sense. It is found that the ground particles from fine grinding facilities exhibit a mechanochemical effect due to severe and high-intensity energy delivered by the grinding mill onto the particles, which led to structural changes at the near surface region where the solids came into contact under mechanical forces.[55] It is believed that, in a jet mill, the energy intensity delivered to the particles was huge, which may result in a mechanochemical effect in the short grinding period.[56] It is thought that, in the grinding process of superfine coal particles, some components in coals may react with oxygen, leading to changes of certain oxygen functional groups under the mechanochemical effects. The smaller the coal particles obtained, the stronger the mechanochemical effects will be exerted. These mechanochemical effects require further investigations. For the moment, it can be concluded that, with the increase of the particle size, there will be fewer organic groups linked to the matrix of the sample, which may result in the decrease of the interfacial thickness.

(54) Huang, X. Y.; Jiang, X. M.; Zhang, C. Q.; Cui, Z. G. *J. Combust. Sci. Technol.* **2009**, *15*, 457–460 (in Chinese).
(55) Venkataraman, K. S.; Narayanan, K. S. *Powder Technol.* **1998**, *93*, 190–201.
(56) Palaniandy, S.; Azizli, K. A. M.; Hussin, H.; Hashim, S. F. S. *J. Mater. Process. Technol.* **2008**, *205*, 119–127.

4. Conclusions

On the basis of the experiments and analysis, the following conclusions can be drawn:

(1) The Porod curves in the high-q region for both NMG and SH coals show a negative deviation from Porod's law, which indicates that there are diffuse interfacial layers for the grains. The gray relational analysis suggests that the coal quality is a main factor influencing the interfacial thickness. The influence of the coal particle size cannot be excluded and is worthy of further investigation.
(2) On the basis of the results of coal pyrolysis investigations in a fixed-bed reactor, it is suggested that, with the increase of the coal quality, the volatile matter decreases due to the decline of the amount of the organic groups. This, in turn, leads to a decrease of the interfacial thickness. Fourier transform infrared (FTIR) spectroscopy was utilized to study the effect of particle size on the functional groups of the coal surfaces. The conclusion is drawn that, with the increase of the particle size, there will be fewer organic groups linked to the matrix of the sample, which results in the decrease of the interfacial thickness.
(3) For the char samples, the interfacial thickness decreases with increasing temperature. Furthermore, the interfacial thickness of NMG chars formed in a CO_2 atmosphere is thinner than that of the chars formed in a N_2 atmosphere.
(4) The effect of inorganic elements on the diffuse interfacial layer of coal particles was studied using the demineralized samples. Results indicate that the demineralized coal particles in the similar experiments show the same trends as the raw coals, but the acid washing process will increase the diffuse interfacial thickness.

Acknowledgment. This work was supported by the National Natural Science Foundation of China (50876060). This work was also supported by the National Academic Award for New Ph.D. Students (2010). The authors thank the beamline BL16B1 (Shanghai Synchrotron Radiation Facility) for providing the beam time.